

GT2011-45+&

THE INFLUENCE OF BLADE SWEEP TECHNIQUE IN LINEAR CASCADE CONFIGURATION

Rosario Spataro
Graz University of Technology
Institute for Thermal
Turbomachinery and
Machine Dynamics
A-8010, Graz, Austria
rosario.spataro@tugraz.at

Gabriele D'Ippolito
Politecnico di Milano
Dipartimento di Energia
Via Lambruschini 4
I-20156, Milano, Italy
gabriele.dippolito@polimi.it

Vincenzo Dossena
Politecnico di Milano
Dipartimento di Energia
Via Lambruschini 4
I-20156, Milano, Italy
vincenzo.dossena@polimi.it

ABSTRACT

One key issue in the advanced aerodynamic optimization of turbomachinery involves the application of 3D blade design techniques. The complex shape of the resulting blades is often a combination of simple techniques such as *sweep*. Such a blade arrangement is often imposed to the designer by structural constraints, space reduction needs, diameter optimization or spanwise blade loading control.

This work aims to study the aerodynamic effects produced on turbine passages by blade sweep; with this term we refer to a configuration where the flow mainstream direction and the blade stacking axis are not orthogonal. A linear cascade of turbine blades, obtained by stacking the same profile with a sweep angle of 20 degrees, was investigated in a blow down facility at an isentropic downstream Mach number of 0.65.

Standing the low aspect ratio of the cascade, the blade was built by simply shifting in axial direction the 2D profile originally used in the reference prismatic blade.

The choice to build the swept blade keeping the same 2D section parallel to the incident flow was considered taking into account the blade low aspect ratio.

Measurements were performed by means of blade surface pressure taps and five holes probe traversing downstream of the cascade; oil and dye flow visualizations were also performed to study the effects on the secondary vortices evolution inside of the passage. Moreover, a commercial CFD code was applied to provide information on the flow field all along the passage.

The same profile was already extensively investigated both by measurements and CFD calculations [1, 2] in order to clarify the effects of blade lean and bowing. This additional paper gives a final contribution addressed to deeply understand the aerodynamic effects produced on turbine cascade flow field by

the separate application of each one of the typical 3D design techniques.

Results from both the experimental and computational investigations are presented and discussed in the paper where a phenomenological approach has been preferred.

Measurements of the blade surface pressure distribution, performed at several blade heights, support the analysis of the pressure field inside of the passage which is mainly based on numerical results. In particular, the paper shows the influence of pressure contours shape on streamwise vorticity inside and downstream of the passage focusing the attention on secondary structures. The downstream vorticity field is then discussed together with the loss distribution in the same region to provide a more exhaustive description.

INTRODUCTION

Swept blades are quite common in nowadays turbomachinery aerodynamics assessment. This part of the blade design process is addressed to control the flow field throughout blade rows in order to maximize the stage performances. A useful tool to reach this goal is given by the application of combined 3D techniques such as sweeping, leaning, compound leaning (bowing) or twisting. Each of these techniques influence the flow field in terms of blade loading and of outflow angle (D'Ippolito *et al* [1]).

Nowadays the blade design is often the output of an optimization process where the 3D shape results in a complex combination of single techniques; since the designer is mainly focused on the overall result, he is not always able to discern what is the role played by each one of these design tools.

Therefore a physical interpretation to qualitatively explain blade lean effects on the flow field was already proposed by the same research group [1] in order to compare two linear cascades mounting the same profile: the first one was composed by prismatic blades (the profile is stacked along an axis normal to the endwall) while the second one is characterized by blades whose profile is still normal to the endwalls, but stacked along a straight leaned axis. The same design methodology is focused in the present work on swept axis blades.

In technical literature it is possible to find different definitions of “sweep”: meridional and true one [3]. Concerning linear cascades with parallel endwalls, this paper will refer to the *meridional sweep* as the angle between the blade stacking axis and the direction normal to the endwalls according to the sketch reported in Figure 1.

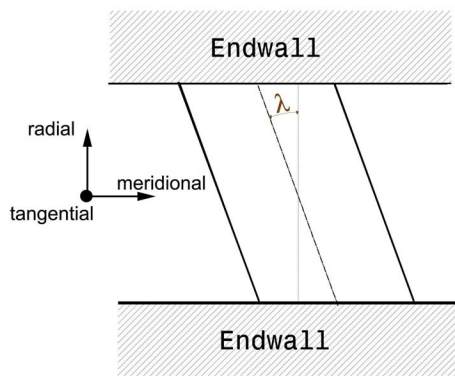


Figure 1 Definition of meridional sweep

A classical application of swept blades can be found in the design of axial steam turbines of intermediate and especially low pressure stages. The large expansion through each stage causes a significant increase of specific volume, so a remarkable flare angle has to be applied to the tip casing. Moreover, it has to be noticed that the streamlines of the actual approaching flow can be skewed with respect to the blade axis, even if the profiles stacking line was designed to be perpendicular to the inlet flow.

Massive application of 3D blade design takes place also in modern aero-engines where several constrains, such as minimizing CO₂ emissions and emitted noise, lead to increase the machine bypass ratio as more as possible. Therefore a continuous growth of the difference between low pressure (LP) and high pressure (HP) stage diameter induces a S-shape flow path in the meridional view. A main consequence is that high swept blades ($\lambda = 40^\circ \div 60^\circ$) can be found in both turbine and compressor.

Pullan discussed the effect of the sweep technique on the blade loading at midspan for the case of a turbine vane *high aspect ratio* in [4]. Referring to a blade section enough far away from endwalls and parallel to the incident flow direction, a modified Zweifel’s loading coefficient was formulated: thus the blade loading can be calculated by means of the velocity

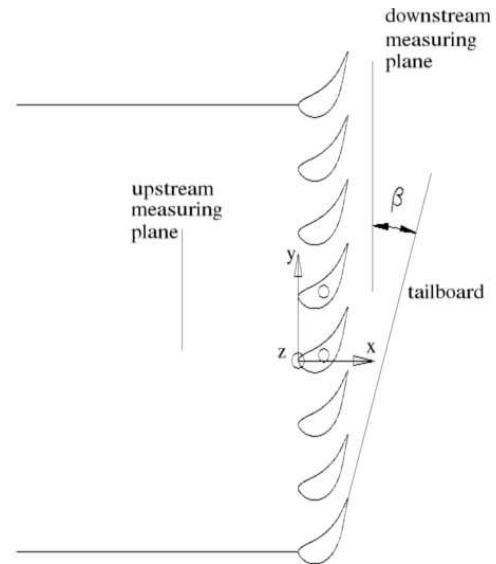


Figure 2 Test section

component normal to blade swept axis. Therefore the cited paper confirmed how, for a blade with high aspect ratio, the right section to be considered for the aerodynamic design is the one normal to the stacking axis.

Many works can be found in open literature and a helpful reference is provided by Gallimore *et al.* [5] who showed how the combined use of the sweep with the dihedral design can increase the stage efficiency of compressor blade rows by controlling the blade loading and therefore reducing regions of inverse flow.

The paper presents the results of a work carried out at the Laboratorio di Fluidodinamica delle Macchine (LFM) of Politecnico di Milano: it represents the final step of a wide research plan focused on both the understanding and the explanation of the flow field effects associated to various basic 3D design techniques.

The aim of this paper is to provide a phenomenological approach that can help to identify the role played by pressure gradients inside the passage and downstream the swept cascade providing a qualitative tool to support designer activity. The effect of blade swept on secondary flows is easily explained and a simple model aiming to qualitatively predict the associated modifications of secondary phenomena is also provided.

NOMENCLATURE

<i>B</i>	axial chord
<i>C</i>	chord
<i>H</i>	blade height
<i>HP</i>	High Pressure
<i>LP</i>	Low Pressure
<i>LE</i>	Leading Edge
<i>M</i>	Mach Number
<i>PS</i>	Pressure Side

- PV* Passage Vortex
Re Reynolds number
S pitch
SS Suction Side
SV Shed Vortex
TE Trailing Edge
x, y axial and tangential coordinates
z coordinate perpendicular to endwalls
 β blade metallic angle (from tangential direction)
 δ secondary deviation ($\delta = \psi - \beta$)
 ψ downstream outlet angle (from tangential direction)
 θ lean angle (from *z*-direction)
 λ blade meridional sweep angle (from *z*-direction)
 ζ local kinetic loss coefficient
 ω flow vorticity

Subscripts

- is* isentropic
TE trailing edge
WK wake projection (on a *x*-constant plane)
SW streamwise

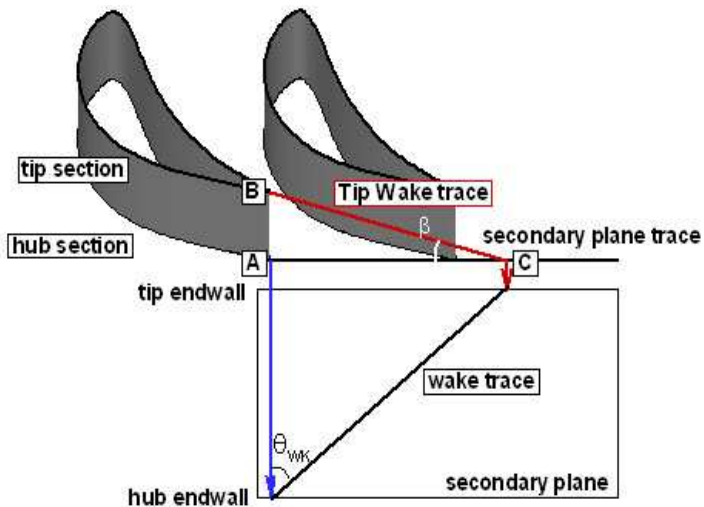


Figure 3 Blade geometry and wake lean definition

EXPERIMENTAL EQUIPMENT

The paper presents the results of an experimental campaign performed on two linear cascades mounting the same 2D profile stacked along different linear axes: for prismatic blades the stacking axis is perpendicular to the endwalls, while for meridional swept blades it bends of 20 degrees (λ in Figure 1). Cascades were tested at the same flow incidence ($i=0$).

The experimental investigation was performed in a blow-down facility located at the LFM. The transonic wind tunnel is fed by 6000 kg of air stocked at 20 MPa. The test section is 50 mm high and 400 mm wide allowing to install 8 blades (Figure 2) which main geometrical parameters are reported in Table 1.

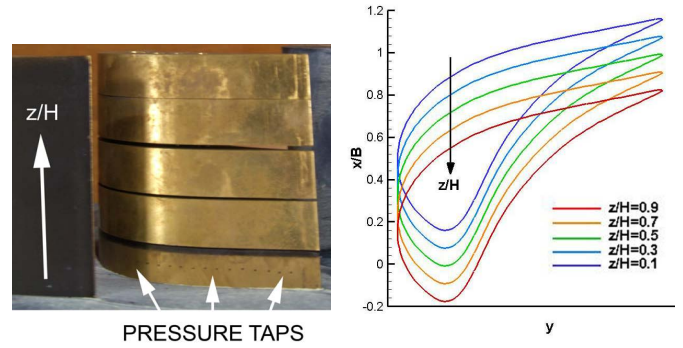


Figure 4 Blade static pressure measurements: arrangement with pressure taps at $z/H=0.1$

Figure 3 shows a 3D view of the cascade evidencing that the meridional sweep of the blade leads to a leaned trailing edge according to:

$$\theta_{TE} = \tan^{-1}(\tan \lambda \cos \beta) \quad (1)$$

where λ and β are respectively the blade sweep angle and the metallic angle of the 2D profile.

In order to obtain a satisfactory 3D periodicity condition, the moveable tailboard located downstream of the cascade was designed with a lean angle in accordance to Equation 1.

Table 1 Blade geometrical characteristics and fluid dynamics parameters

Blade Chord <i>C</i> [mm]	60
Axial Chord <i>B</i> [mm]	43.3
Blade Height <i>H</i> [mm]	50
Pitch – Chord ratio <i>S/C</i>	0.8
Metallic Angle β [deg]	15
Sweep Angle λ [deg]	20
Stagger Angle γ (from <i>y</i> direction)	42.5
Design Reynolds number	$0.88 \cdot 10^6$
Design Mach number	0.65

Flow measurements were performed by traversing a five hole probe with a head diameter of 1.8 mm on a plane located at 50 percent of the axial chord downstream the cascade (“measuring plane” in Figures 2 and 6). The probe was calibrated in the range ± 25 deg and ± 16 deg in yaw and pitch angles respectively and for Mach number ranging from 0.2 up to 1.4. The estimated probe accuracy for static and total pressure is $\pm 0.5\%$ of the dynamic pressure, while for flow angle measurement is ± 0.2 degrees.

A prismatic 3 hole probe and a thermocouple were used for a continuous monitoring of inlet total pressure and temperature.

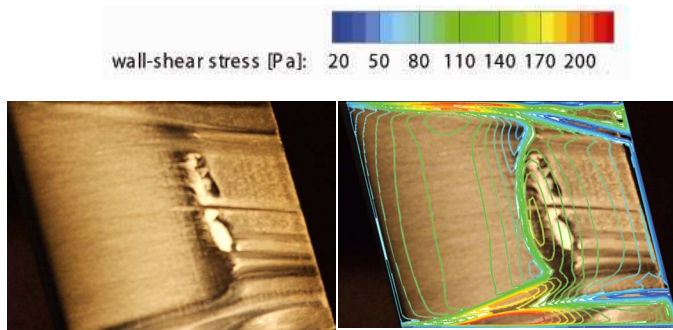


Figure 5 Oil and dye surface flow visualization on blade suction side and superimposition with computed wall shear stress

In order to provide proper CFD inlet boundary conditions, a miniaturized total pressure probe was traversed in the upstream boundary layer.

The cascade central blade was instrumented with 40 pressure taps of 0.4 mm diameter (25 on suction side and 15 on the pressure side) located along the original profile, which means on a section parallel to the endwalls. Since the effect of the sweep extends along the blade height, the instrumented swept blade was built with a particular arrangement. It consists in piling up a certain number of blade slices as pictured in Figure 4, where a small gap between different slices was left in order to clarify the blade setup. Therefore, the radial location of the instrumented section can be moved towards hub or tip by adding or removing slices respectively: measurements were performed at five different spanwise positions: $z/H=0.1, 0.3, 0.5, 0.7, 0.9$.

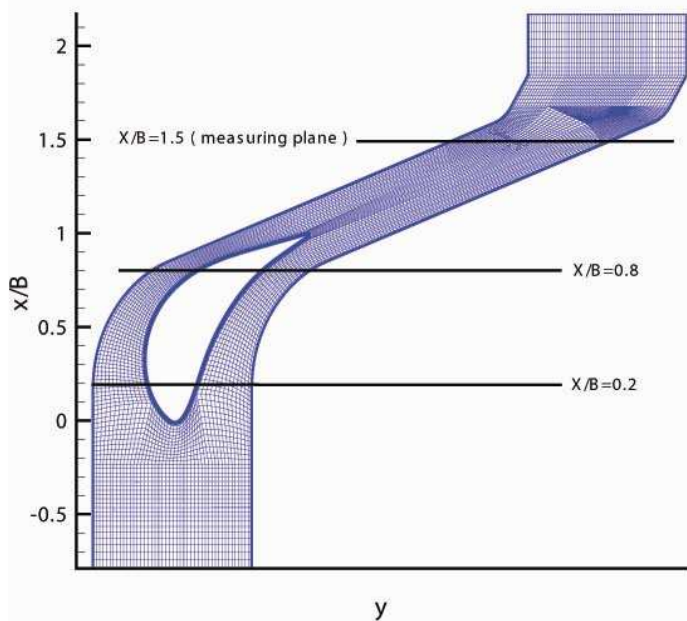


Figure 6 2D mesh at midspan

Flow Visualization

Oil flow visualizations were performed by using a combination of oil, diesel and Ruthilium (TiO_2). With such a mixture it is possible to obtain a map of wall shear stress, providing an accurate picture of the flow onto blades and endwalls.

Visualization results are a useful reference to check CFD code reliability in reproducing and correctly locating main flow structures. An example of such a comparison is reported in Figure 5 where a superimposition of test picture and calculated wall shear stress map, reveals a remarkable accordance between the two result sets.

NUMERICAL TECHNIQUES

The numerical investigation was performed by means of a commercial CFD code (Fluent[®]). The closure of the RANS system was set with a $k-\omega$ turbulence model in the Shear Stress Transport formulation.

The 2D mesh topology (Figure 6) adopted for this work is the same applied for previous investigation in [1] and [2] as resulting from grid dimension sensitivity analysis. The overall domain results to be splitted in subdomains meshed with H-type grid except for the one adjacent the blade where O-type grid was used.

The 3D mesh is obtained by stacking the same 2D mesh along the blade axis and the overall size consists of 1.5 million hexahedral cells. The y^+ was kept below 1 onto the blade and below 2 onto the endwalls.

Inlet and outlet boundaries were located respectively at $x/B=-0.75$ and $x/B=2.2$ to avoid boundary effects influence on the flow field.

According to experimental measurements, a total pressure profile along channel height and constant total temperature were imposed at the inlet, while averaged static pressure value was set for the outlet condition (Table 2).

Table 2 Boundary conditions

Inlet	Total Pressure (average) [Pa]	130000
	Total Temperature [K]	300
	Turbulent Intensity [%]	3
	Turbulent Viscosity Ratio [-]	0.1
Outlet	Static Pressure (average) [Pa]	88200

RESULTS PRESENTATION

In the first part of this section the influence of the sweep angle on the blade loading will be discussed by considering CFD results carried out on both blades for the design Mach number of 0.65.

The second part of the section is dedicated to the understanding of the flow field development through the linear

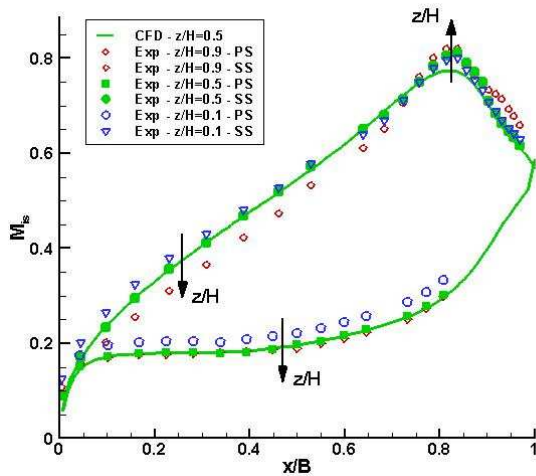


Figure 7 Isentropic Mach number distribution at three blade heights

cascade mainly making use of numerical data, thanks to their higher spatial resolution. The influence of sweep on secondary structures downstream the cascade will be discussed providing a comprehensive analysis of the main phenomena influencing turbomachinery aerodynamic design.

Surface Isentropic Mach number distribution

Five planes have been analyzed ($z/H=0.1, 0.3, 0.5, 0.7, 0.9$) in order to investigate the effects of sweep on the surface isentropic Mach number distribution along the blade height. The charts are plotted along the non dimensional axial chord and every distribution is referred to the correspondent profile leading edge in order to improve plots readability and comparison; therefore all plots have been shifted to the same axis origin.

Figure 7 shows the comparison between measured and computed Mach number distributions along the axial chord at

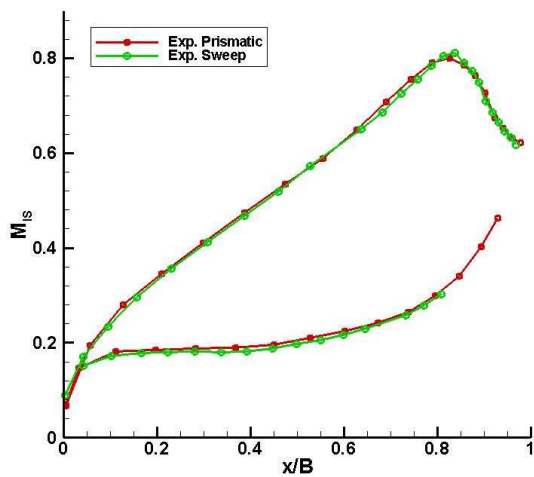


Figure 8 Profile M_{is} comparison between prismatic and swept blades at midspan

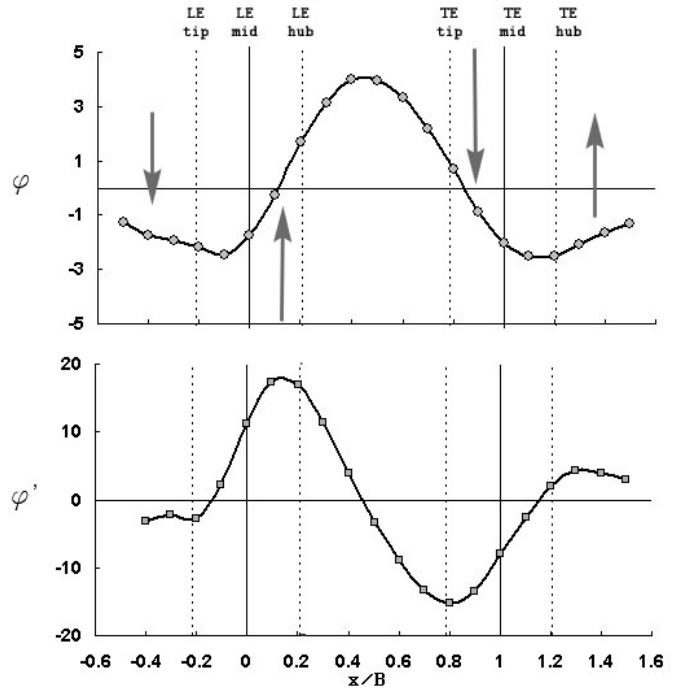


Figure 9 ϕ and ϕ' along meridional direction

midspan. It is possible to appreciate a good agreement between experimental and numerical data. The same figure also reports experimental isentropic Mach number distributions close to the endwalls ($z/H=0.1, 0.9$) evidencing the same trend already observed in [3]. As well known, sweep technique application alters the blade loading along the span. In particular, keeping midspan section as a reference, the forward sweep in analysis leads to a more aft-loaded tip profile and a more front loaded hub one. The Mach number distribution differences along the span are not remarkable because of the low blade aspect ratio, as better detailed in the following.

A comparison with CFD results was here restricted to mid span section because their reliability close to the endwalls is critical as already shown by Potts [6].

Figure 8 shows the comparison of isentropic surface Mach number at midspan for the prismatic and the swept cascade. The two charts are almost the same, confirming that for low aspect ratio blades, the flow stream surfaces differ from the one expected in the case of infinite blade length. Moreover, in this case, the correct aero-design has to be based on a section parallel to the endwalls. Therefore the idea that the profile defining the actual loading is the one normal to the stacking axis (Smith and Yeh [7]) results to be not realistic for a such low aspect ratio blade .

Flow Passage

A detailed analysis of the general behaviour of the flow throughout the cascade is reported in this section.

The discussion will be based on CFD results and different planes at various meridional positions were extracted to support the subsequent analysis.

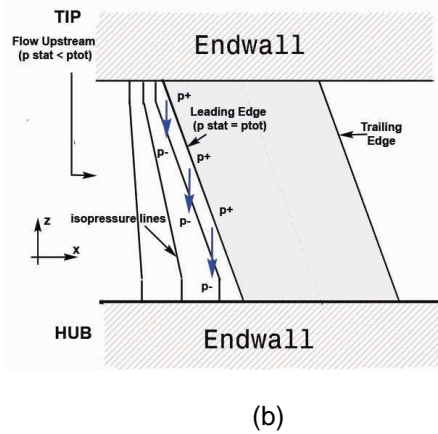
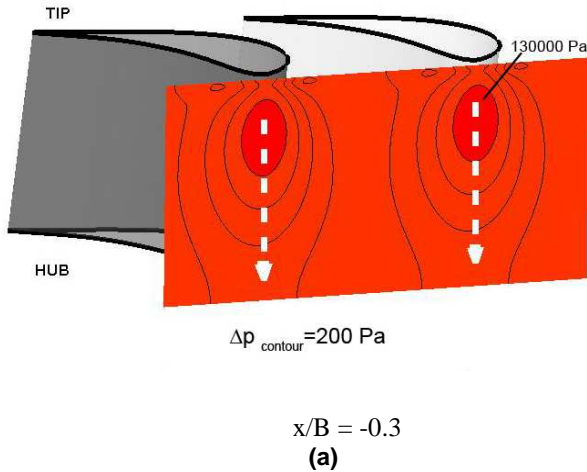


Figure 10 Effect of a swept blade on the upstream flow field

It is interesting to start the flow field analysis by introducing the two coefficients defined in equations 2 and 3:

$$\phi(\hat{x}) = \frac{\bar{V}_z}{\bar{V}} \cdot 100 \Big|_{\hat{x}} \quad (2)$$

$$\phi'(\hat{x}) = \frac{d\phi}{dx} \Big|_{\hat{x}} = \frac{\phi_{i+1} - \phi_{i-1}}{x_{i+1} - x_{i-1}} \Big|_{x_i = \hat{x}} \quad (3)$$

The first coefficient defines the ratio between the mass averaged z-Velocity and Velocity magnitude, while the second one is the first one derivative.

Figure 9 reports the meridional trend of ϕ and ϕ' from far upstream to far downstream. The idea is to provide an overall description of 3D effects induced by the blade sweep through the passage. The attention is focused on radial normalized velocity and acceleration, where the second is proportional to radial forces. This approach was already applied for the lean technique in [1] where the ϕ coefficient was plotted and discussed.

Figure 9 will be taken as reference for the following physical analysis.

a) Upstream flow

Frames in Figure 10 show the effects of the sweep on the upstream flow field by considering CFD results. Frame *a* reports pressure contours on a plane located at $x/B = -0.3$, while Frame *b* reports a sketch in order to clarify the sweep induced pressure gradient upstream of the cascade.

The 3D shape of the blade clearly produces a pressure gradient generated by the flow stagnation on the blade leading edge. Pressure contours plots are reported in Figure 10(a) together with the indication of the thrust acting on the flow represented by means of white arrows. As sketched in Figure 10(b), pressure contours lie on secondary planes enough far upstream, but they tend to align with blade axis while approaching the blade leading edge.

b) Blade passage

In this section the effects of the pressure gradients generated by the sweep in the blade channel are presented and discussed in terms of:

- induced radial forces pushing the flow spanwisely and along z-direction
- pressure contour maps
- loss and vorticity field downstream the cascade.

Figure 11a reports computed pressure contours onto blade suction side, while Figure 11b reports pressure contours onto blade pressure side. The swept blade under analysis is characterized by a low aspect ratio, typical of middle and high pressure steam turbine; as a consequence, the effects of blade sweep are as more emphasized as the aspect ratio increases, so more significant boundary effects have to be expected with respect to blades with higher aspect ratio. In Figures 11a and 11b it is possible to observe how pressure contours are anyway approximately aligned with swept blade axis in the midspan region. The difference from infinite blade is here due to the pressure contours bending approaching the endwalls. The boundary effects now forces pressure contours to bend close to the endwall assuming a direction almost perpendicular to hub and tip surfaces in the front part of the blade. This effect extends quite far from the endwall reducing the overall influence of sweep design.

White arrows in Figures 11a and 11b indicate the direction of the thrust on the flow close to leading and trailing edges, typical phenomenon of any kind of swept blade. This action on the flow is in accordance to the ϕ coefficient trend showed in Figure 9. Moreover, the two grey arrows spanwisely oriented indicate the thrust on the flow close to the blade surfaces due to sweep effects. This acceleration will influence the wake vorticity at the trailing edge, because a mismatch in spanwise velocity takes place between the two blade sides. As a consequence, the shear layer just downstream the blade trailing

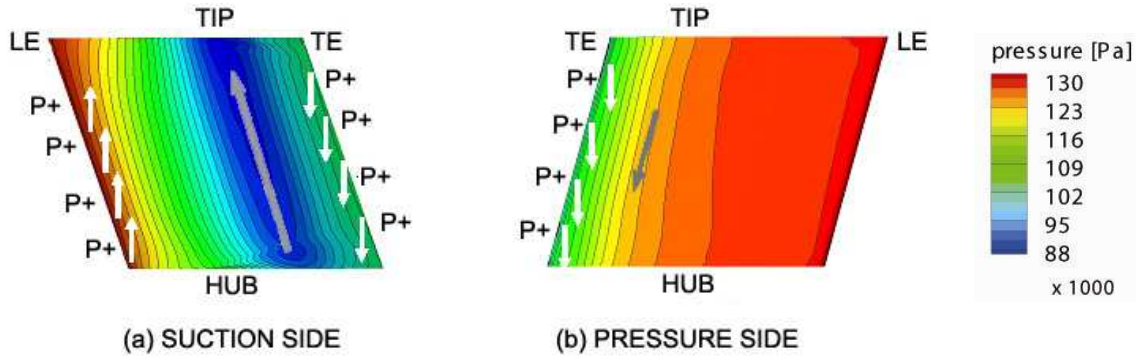


Figure 11 Surface pressure distribution of the suction and the pressure sides

edge is enhanced by the sweep geometry, as it will be better clarified in Figure 15.

Profile pressure distributions at different blade heights are reported in Figure 12, where again the sweep design influence on profile loading can be noticed. Tip section appears to be aft- and lower loaded, while hub is slightly more front loaded. The spanwise pressure variation between hub and tip can be obtained from Figure 12 by the difference between the distribution at $z/H = 0.9$ and $z/H = 0.1$ evaluated by keeping constant the x/B coordinates. It is important to observe that spanwise pressure difference between hub and tip is opposite on pressure and suction sides. In particular: on the suction side the spanwise pressure difference reaches about 2000 Pa at $x/B = 0.8$ and the related thrust on the flow is hub-to-tip oriented, while on pressure side the spanwise pressure difference reaches about 1800 Pa at $x/B = 0.8$ but now the related thrust on the flow is tip-to-hub oriented. This effect is in accordance to the previous observation supported by grey arrows in Figure 11.

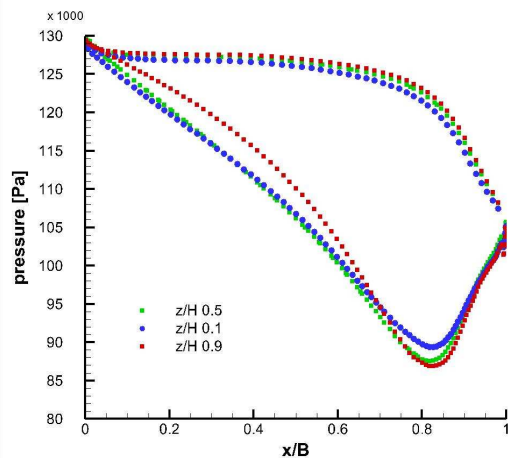


Figure 12 Blade pressure distributions at different blade heights

Figure 13 reports the pressure distribution on secondary planes located at $x/B=0.2$ and $x/B=0.8$ (x/B evaluated at midspan section and corresponding respectively to the physical extension of the passage, i.e. hub leading edge and tip trailing edge). Plane locations are chosen in order to make plane pass for hub leading edge ($x/B=0.2$) and tip trailing edge ($x/B=0.8$). White arrows help to appreciate how the spanwise pitching of the flow is controlled by the gradients in z -direction and for the plane located at $x/B = 0.8$ a vertical red line evidences how pressure contour bending produces the thrust on the flow tip-to-hub oriented. Finally, downstream of the trailing edge it takes

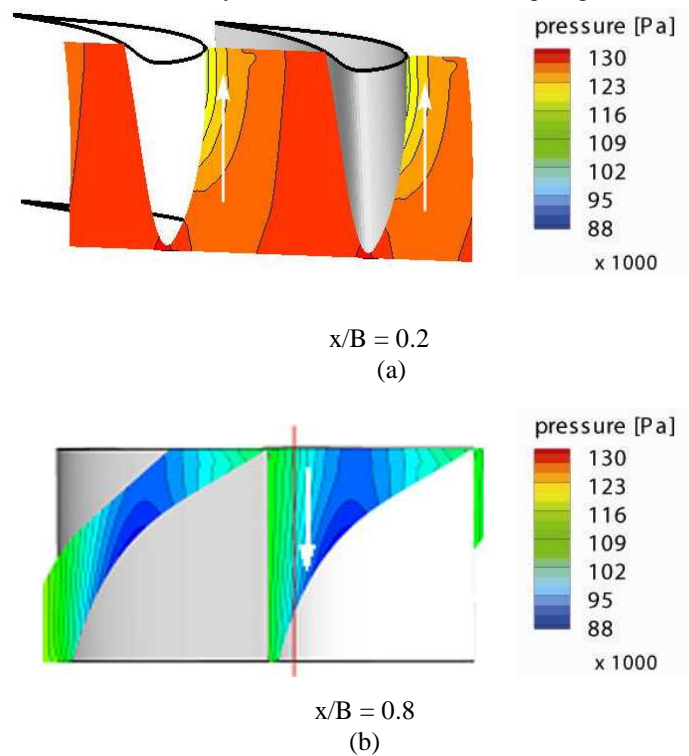


Figure 13 Effect of a swept design on the main flow. (a) View from upstream - Pressure contours on a plane located at $x/B=0.2$. (b) View from downstream - Pressure contours on a plane located at $x/B=0.8$

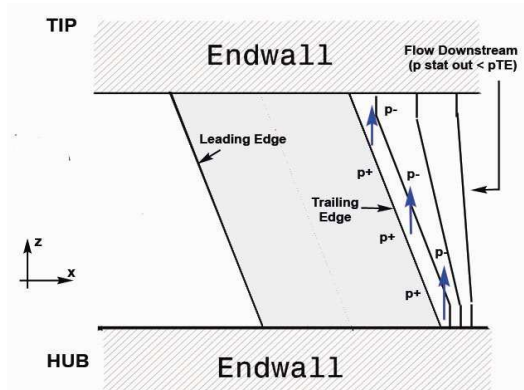


Figure 14 Effect of the sweep on the flow field downstream the cascade

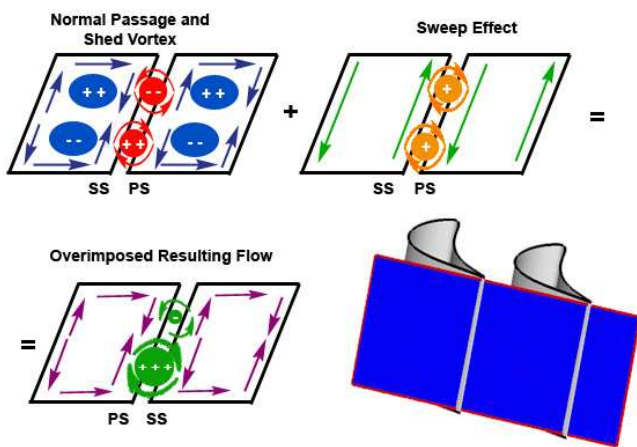


Figure 15 Effects of the sweep design on vorticity downstream

place the same physical scheme proposed upstream of the leading edge, as Figure 14 demonstrates. The thrust on the flow changes its sign again pushing low flow energy fluid towards the midspan region as it will be evidenced in subsequent discussion.

Table 3 CFD Mass Averaged Yaw Angle

$\bar{\psi}$	Prismatic [deg]	17.38
$\bar{\psi}$	Swept [deg]	18.50

c) Downstream flow

The discussion on the downstream flow field is supported by the analysis summarized in Figure 15, that clarifies how spanwise pressure gradients can influence the vorticity generation downstream.

The first frame reproduces a view from downstream of a typical vorticity scheme in which passage vortices (blue circles) and shed vortices (red circles) are evidenced. Positive streamwise vorticity sign in these views corresponds to clockwise rotation sense. The application of sweep technique

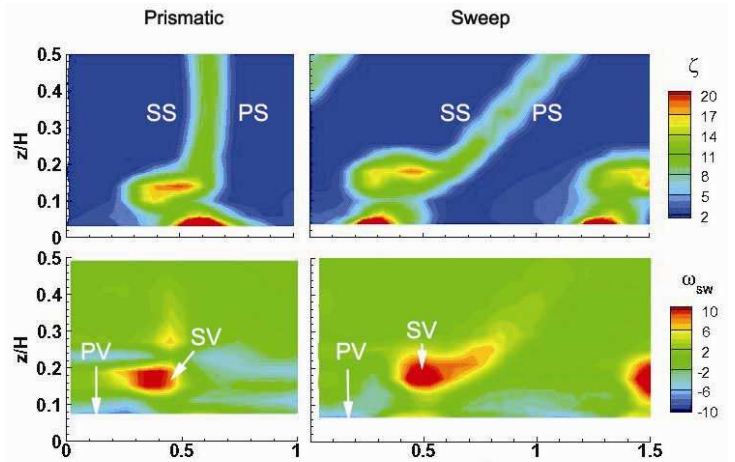


Figure 16 Experimental data: Effect of the sweep on the generation of the downstream loss and vorticity fields on a plane at $x/B=1.5$ from midspan

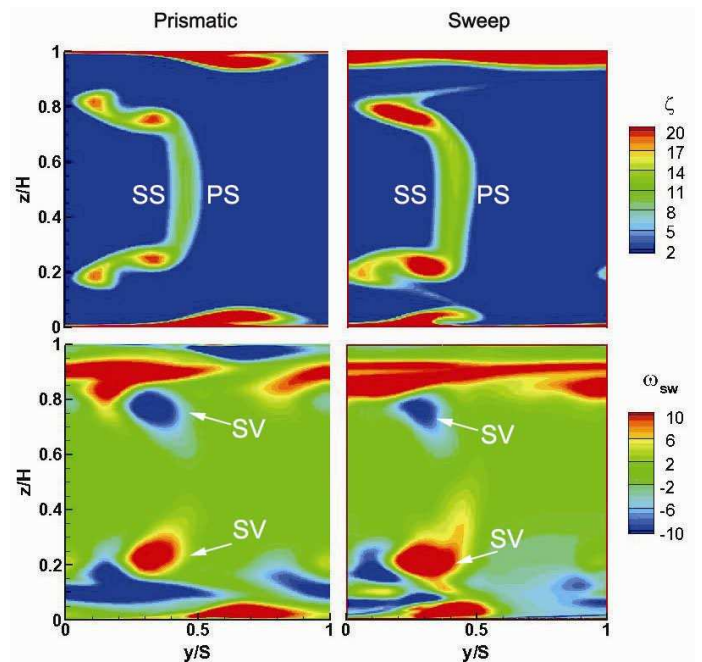


Figure 17 CFD: Effect of the sweep on the generation of the downstream loss and vorticity fields on a plane at a fixed distance of $0.5 x/B$ from the blade trailing edge.

produces spanwise directed flows close to blade surfaces in the trailing edge region, as previously observed in the analysis summarized in Figure 11. By assuming a separation of the effects (just for descriptive reasons), immediately downstream the trailing edge these two opposite oriented flows get in contact producing a shear layer as sketched in the second frame. The overall result is a sort of superimposition of vorticity magnitudes; in particular, in the hub region the two shed vorticity are characterized by the same sign, then the overall

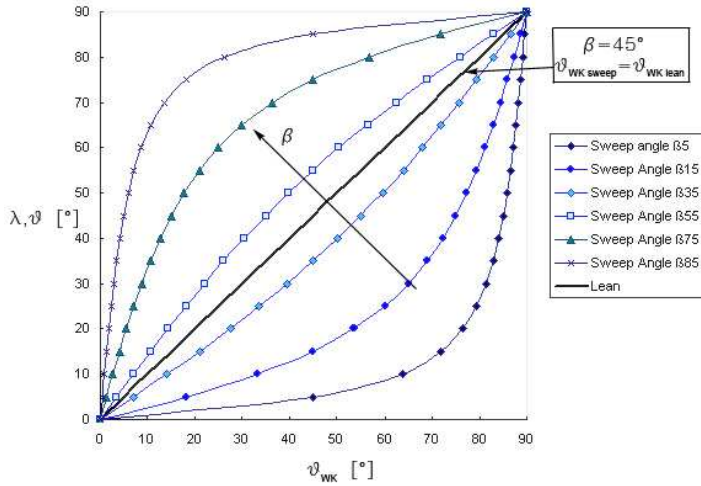


Figure 18 Wake inclination by the use of lean and sweep technique

result is a vorticity strengthen. In the tip region the opposite feature takes place because the two vorticity have opposite sign.

Observations drawn until now are confirmed by experimental data reported in Figure 16 showing measurement performed on a plane at $x/B = 1.5$ (x/B evaluated with respect to midspan). Loss and vorticity cores for the swept cascade flow field are more shifted towards midspan than in the prismatic condition supporting the analysis of pressure gradient at the trailing edge previously presented. Moreover, shed vorticity core is stronger and larger than for the prismatic blade, supporting the model just above proposed.

Figure 17 reports computed maps of losses and streamwise vorticity for prismatic blade (left) and swept blade (right) respectively. Results for the swept blade only are reported on a plane defined by the tangential direction and a direction parallel to the swept trailing edge. The plotting plane is then swept with respect to the axial direction. As a consequence the trailing edge distance from the plane represented in Figure 17 is now constant along the whole blade height for both cascades; furthermore, the two cases experiences the same mixing effect on wake losses and streamwise vorticity.

It is possible to notice the higher loss level in the wake for the swept blade than for the prismatic one, supporting the action of the sweep induced shear layer just downstream the trailing edge; furthermore, the vorticity map supports the difference in vorticity magnitude and extension between the hub half channel and the tip one for the swept blade. Swept blade downstream vorticity can be roughly obtained from the prismatic one by adding a positive contribution, which is exactly the sweep induced effect presented in Figure 15 and above discussed.

The sweep design on one hand reduces the flow deflection (see Table 3), while on the other hand loss cores values and extension are increased because of the stronger mixing process downstream of the trailing edge, even by keeping unchanged both the profiles and the inlet boundary layer.

It is interesting to notice how, keeping both the profiles and the inlet boundary layer unchanged, the sweep design reduces the flow deflection (see Table 3), but meanwhile loss cores values and extension are increased because of the stronger mixing process taking place downstream of the trailing edge.

Wake inclination downstream the cascade

Figure 16 shows another consequence of sweep application: as for leaned blades, the blade wake trace on a conventional secondary plane (tangential-radial) results inclined with respect to the radial direction. This can be very important from the point of view of the turbine engineer, in order to design the downstream stage. The simple geometrical relation reported in Equation 4 can be used as a first approximation with the aim to calculate the wake mean leaning angle downstream of a swept blade. Equation 4 has been derived under the hypothesis of constant exit angle along the span:

$$\theta_{WK\ sweep} = \tan^{-1}\left(\frac{\tan \theta_{TE}}{\sin \beta}\right) = \tan^{-1}\left(\frac{\tan \lambda}{\tan \beta}\right) \quad (4)$$

In the simplified model summarized in Equation 4, the exit angle has been substituted with the corresponding metallic one (β), but more complex expressions based on geometrical considerations or predictive criteria can be used for improving the prediction accuracy.

Furthermore, it is easy to verify that the leaning angle of the blade corresponds to the lean angle of its wake ($\theta_{WK\ lean} = \theta$). In Figure 17 the functions for the evaluation of the wake leaning angle for leaned and/or sweep blades are plotted.

In particular Equation 4 shows that, in the case of a swept blade, the inclination of the wake is a function of two variables: the sweep angle λ and the metallic angle β at the trailing edge. By composing Equation 4 and 5 under the same hypothesis of constant angle along the span, it is possible to carry out a general formulation in the case of lean and sweep combined design:

$$\theta_{WK} = \theta + \tan^{-1}\left(\frac{\tan \lambda}{\tan \beta}\right) \quad (5)$$

In real conditions, secondary deviation effect has to be kept into account, so that the metallic angle in equation above will be replaced by the actual flow angle which is a function of the spatial coordinates. Therefore Equation 5 will be reformulated as follows:

$$\theta_{WK} = \theta + \tan^{-1}\left(\frac{\tan \lambda}{\tan \psi}\right) \quad (6)$$

CONCLUSIONS

The paper shows the results of an experimental and numerical investigation aimed to provide a phenomenological

explanation of the sweep effect in the 3D turbine blade design, with particular reference to low aspect ratio cascades.

In order to isolate the sweep effect from others, the investigation was performed on linear cascade; so acting, the superimposition of annular effects with the natural radial pressure gradient is avoided. The work is addressed to the understanding of flow phenomena by applying a qualitative model already employed for the blade lean study. Swept blade was compared with prismatic one and data reduction provided results in accordance to literature references.

As a first step, it was reminded that the sweep design induces forces orthogonal to the approaching flow and the study of the mass averaged flow velocity along z-direction and its derivative evidenced the primary role played by pressure gradients on secondary planes on the flow pitching.

The second step reports the discussion of flow field close to the blade surfaces revealing an opposite sign of the pressure gradient, which influences mainly the wake development in terms of losses and vorticity. Great attention was focused on blade suction side, also evidencing how the presence of the endwalls affects the pressure distribution on the blade surface close to tip and hub, inducing spanwise pressure gradients. Their effects can be clearly noticed by observing the spanwise variation of the blade loading and by comparing prismatic and swept blade vorticity maps downstream the cascade.

The sweep-induced flows close to blade surfaces produce a shear layer which interacts with natural vorticity development just downstream of the trailing edge. In particular shed vorticity and loss is strengthened by 3D design, in spite of the overall deflection is lower than for the prismatic cascade.

Finally the inclination of the wakes downstream the blade was observed and a geometrical relation was proposed to easily estimate the wake leaning angle in case of combined lean-sweep design.

The approach employed in this paper pointed out again the importance of pressure field on 3D blade flow development, suggesting a qualitative model to evaluate the downstream consequence of a simple sweep design technique.

ACKNOWLEDGMENTS

The authors wish to thank Franco Tosi Meccanica SpA for providing blade profile data. The authors would also like to thank Claudio De Ponti for the contribution to the experimental campaign.

REFERENCES

- [1] D'Ippolito G., Dossena V., Mora A., "The influence of blade lean on straight and annular turbine cascade flow field", J Turbomachinery 2011, vol 131
- [2] Mora A., D'Ippolito G., Dossena V., "On the application of leaning technique on annular turbine", ISROMAC12-2008-20031
- [3] Pullan G., Harvey N.W., "The influence of sweep on axial flow turbine aerodynamics in the Endwall Region", J Turbomachinery 2008, vol 130
- [4] Pullan G., Harvey N.W., "The influence of sweep on axial flow turbine aerodynamics at Midspan", J Turbomachinery 2007, vol 128

[5] Gallimore S.J., Bloger J.J., Cumpsty N.A., Taylor M.J, Wright P.I., Place J.M.M., "The use of Sweep and Dihedral in Multistage Axial Flow Compressor Blade – Part II: Low and High Speed Designs and Test Verification", J Turbomachinery, vol 124, pagg 533-541

[6] Potts, I., 1987, "The Importance of S-1 Stream Surface Twist in the Analysis of Inviscid Flow Through Swept Linear Turbine Cascades," Proc. Inst. Mech. Eng., Part C: Mech. Eng. Sci., 258_87_, pp. 231–248.

[7] Smith, L. H., and Yeh, H., 1863, "Sweep and Dihedral Effects in Axial-Flow Turbomachinery," ASME J. Basic Eng., 85, pp. 401–416.

[8] Harrison S., 1880, "The influence of blade lean on turbine losses", ASME Paper 80-GT-55

[9] A. J. Cooper, N. Peake, "Rotor-Stator Interaction Noise in Swirling Flow: Stator Sweep and Lean Effects", 2006, AIAA JOURNAL, Vol. 44, No. 5.